Supporting Information for "The characteristics of mesoscale convective system rainfall over Europe"

Nicolas A. Da Silva [1], Jan O. Haerter[1,2,3]

[1]Complexity and Climate, Leibniz Centre for Tropical Marine Research, Fahrenheitstrasse 6, 28359 Bremen, Germany

[2]Physics and Earth Sciences, Constructor University Bremen, Campus Ring 1, 28759 Bremen, Germany.

[3]Niels Bohr Institute, University of Copenhagen, Blegdamsvej 17, 2100 Copenhagen, Denmark.

Contents of this file

Introduction This document presents supporting figures for "The characteristics of mesoscale convective system rainfall over Europe". It provides the probability density function (PDF) of the goodness of ellipse fit (G) for mesoscale convective systems (MCS; Fig. S1) and the precipitation seasonal climatology (Fig. S4) from the Integrated Multi-satellitE Retrievals for GPM (IMERG) product. It describes an alternative MCS detection method using the Convective Available Potential Energy (CAPE) instead of lightning occurrence (Text S1; Fig. S3). It contains the analogous figures to the main manuscript but for other types of precipitation features (PF; isolated convection and stratiform) for total precipitation (Fig. S6, S7), the contribution to extreme precipitation (Fig. S10, S11, S5), the precipitation/lightning diurnal cycle (Figs S13, S16, S12, S15, S14, S17).

———

April 10, 2023, 12:09pm

Text S2 and Figs S8, S9 support the coastal maximum of precipitation found in the main manuscript (Figs S8, S9). Finally, this document provides with the frontal pixel frequency as a function the distance for different PF types (Fig. S18).

Text S1: sensitivity to convection classification. Lightning occurrence within a precipitating system provides a clear indication for convection. However, lightning data are subject to measurement error and not continuously available in all regions. Thus, and to assess the robustness of our results, we tested an alternative criterion, namely CAPE determined from ERA5. We first determined an optimal threshold for ERA5 CAPE above which a PF is considered convective by additionally using the surface synoptic observations (SYNOP; O'Brien (2008)) dataset: whenever a cumulonimbus, thunderstorm, or lightning strike was observed at a given SYNOP station and at least 50 other SYNOP stations located within a radius of 500 km around this station (as evidence of convective activity), we extract the nearest ERA5 grid point and construct a PDF of ERA5 CAPE. The ERA5 CAPE field was previously filtered over a 5 x 5 spatial window in which the maximum CAPE was retained. By comparing the exceedance probability of CAPE in the occurrence of convection with the exceedance probability of CAPE for all the concatenated time series of all stations, we determine an optimal threshold of $100 \, \mathrm{J.kg^{-1}}$ above which the difference between both the former and later exceedance probabilties do not increase anymore (Fig.S2). With this alternative identification method, at any time of its life cycle, if a PF contains (or is surrounded in a 5-km radius) an ERA5 CAPE pixel value exceeding $100 \, \mathrm{J.kg^{-1}}$, then this PF is defined as convective. We then use the same diameter and duration thresholds (see section 2 of the main manuscript) to define MCS PFs. With this alternative method we find a similar spatio-temporal distribution of MCS

precipitation over Europe (Fig. S3), exhibiting peaks in the same areas as those noted in section 3, which shows that the locations of high MCS activity are robust.

Text S2: coastal effect.

Figs. S9 and S8 were drawn to provide insights on the local maximum of precipitation found in coastal areas and described in the main manuscript. They show the monthly anomalies of surface water vapor mixing ratio and wind conditioned on MCS or isolated convection occurrence (respectively) near the coasts in December in four coasts around Europe. The occurrence of a MCS (respectively isolated convection) coastal event was defined by considering the spatial sum of MCS (resp. isolated convection) hourly precipitation heights within a box along the coast (drawn in magenta) and selecting hourly events for which this total precipitation height exceeds a threshold of 10 mm. Fig S8 shows pronounced wind and moisture anomalies converging to the coasts, and associated precipitation along the coasts. Fig S9 generally shows similar patterns but with a more diverted flow by the coast. While the coasts of Netherlands and Germany are still an area of low level wind convergence for MCS events (Fig S9b), there is an overall inland wind anomaly, which constitutes an exception compared to the other locations.

References

O'Brien, C. (2008). *Met office (2008): Land synop reports from land stations collected by the met office metdb system.* `https://catalogue.ceda.ac.uk/uuid/9f80d42106ba708f92ada730ba321831`. (Online; accessed 21 October 2021)

:
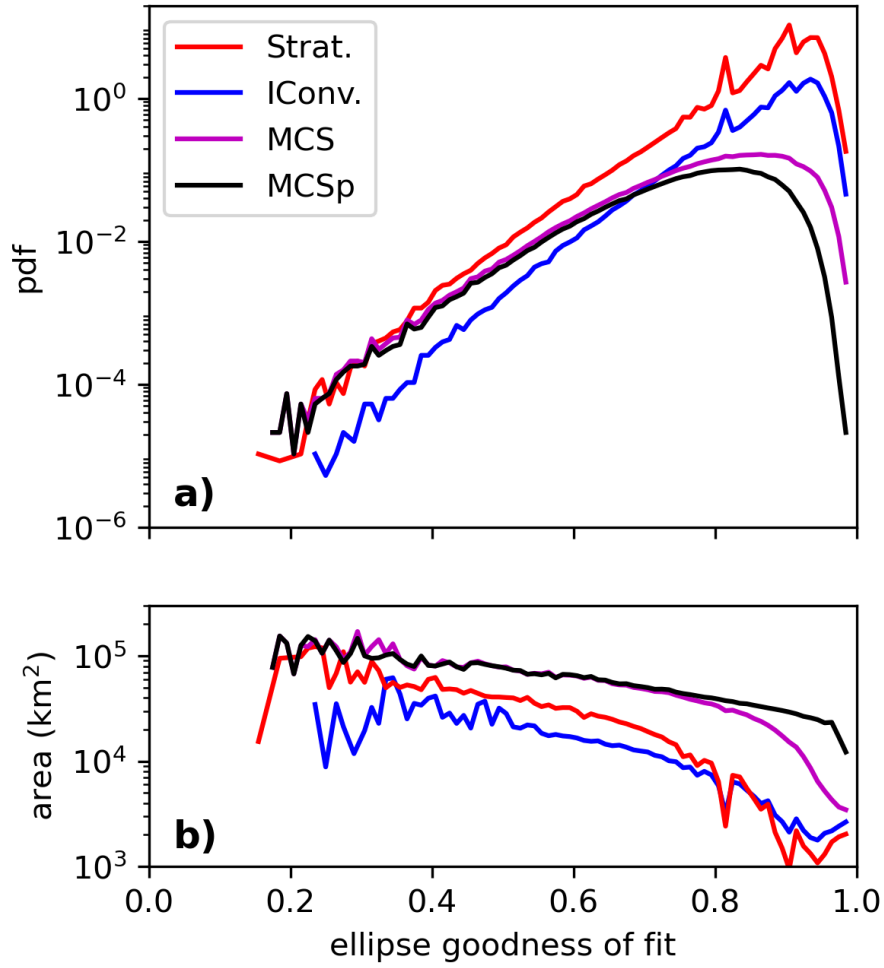
Figure S1. Probability Density Functions (PDF) of the ellipse Goodness of fit (G) as defined in eq. 1 in the main manuscript (a) and PF Area as a function of G for stratiform (”Strat.”, red), isolated convective (”IConv.”, blue), MCS (magenta) PFs, and for MCS periods (”MCSp”, black; b). MCSp was built by selecting only instants for which a MCS PF has MCS attributes (see section 2a of the main manuscript). The PDF (in a) were normalized by the total number of PF.
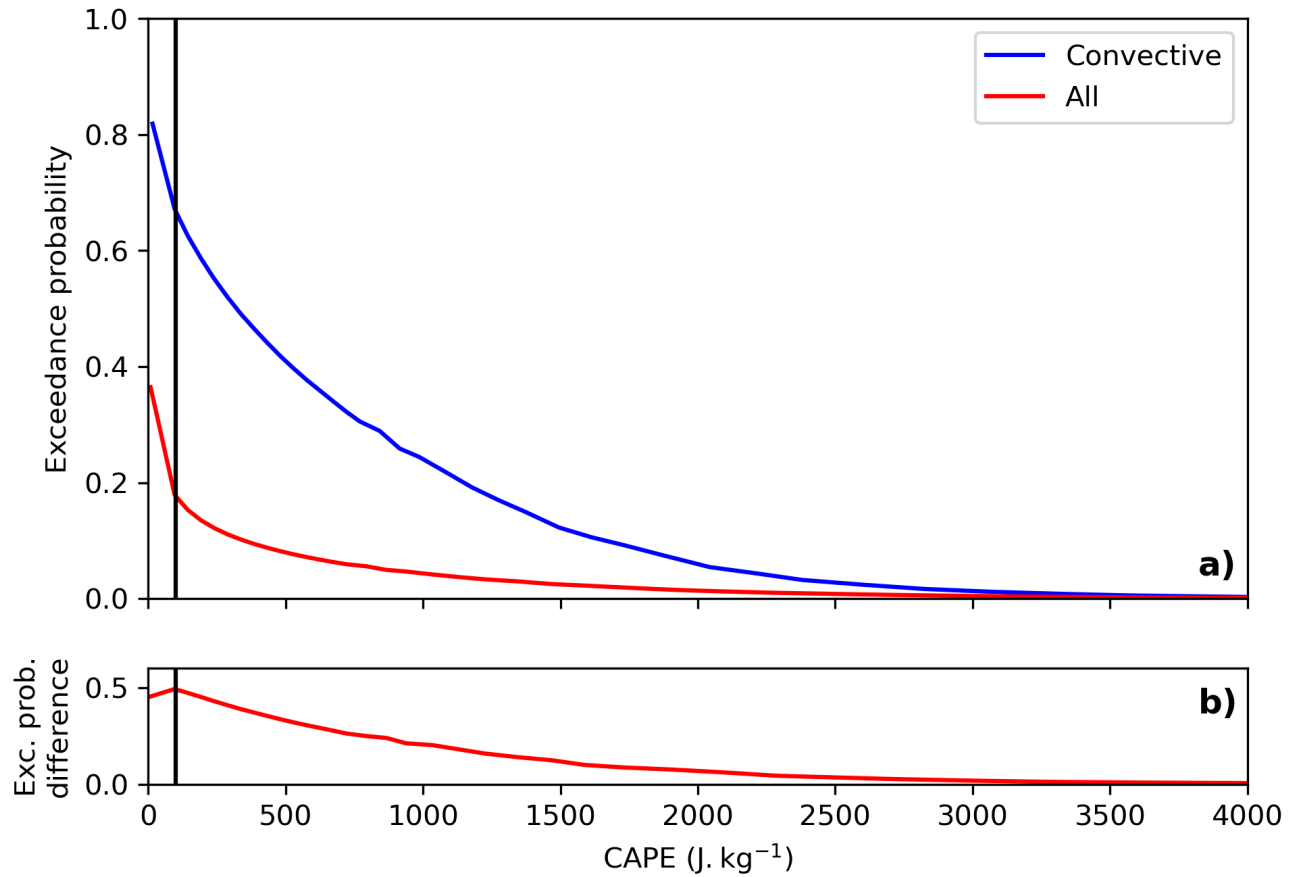
Figure S2. Exceedance probability of Convective Available Potential Energy (CAPE) for SYNOP convective observation events (blue), and for all observation events (red; a) and their difference (b) as a function of CAPE.

April 10, 2023, 12:09pm
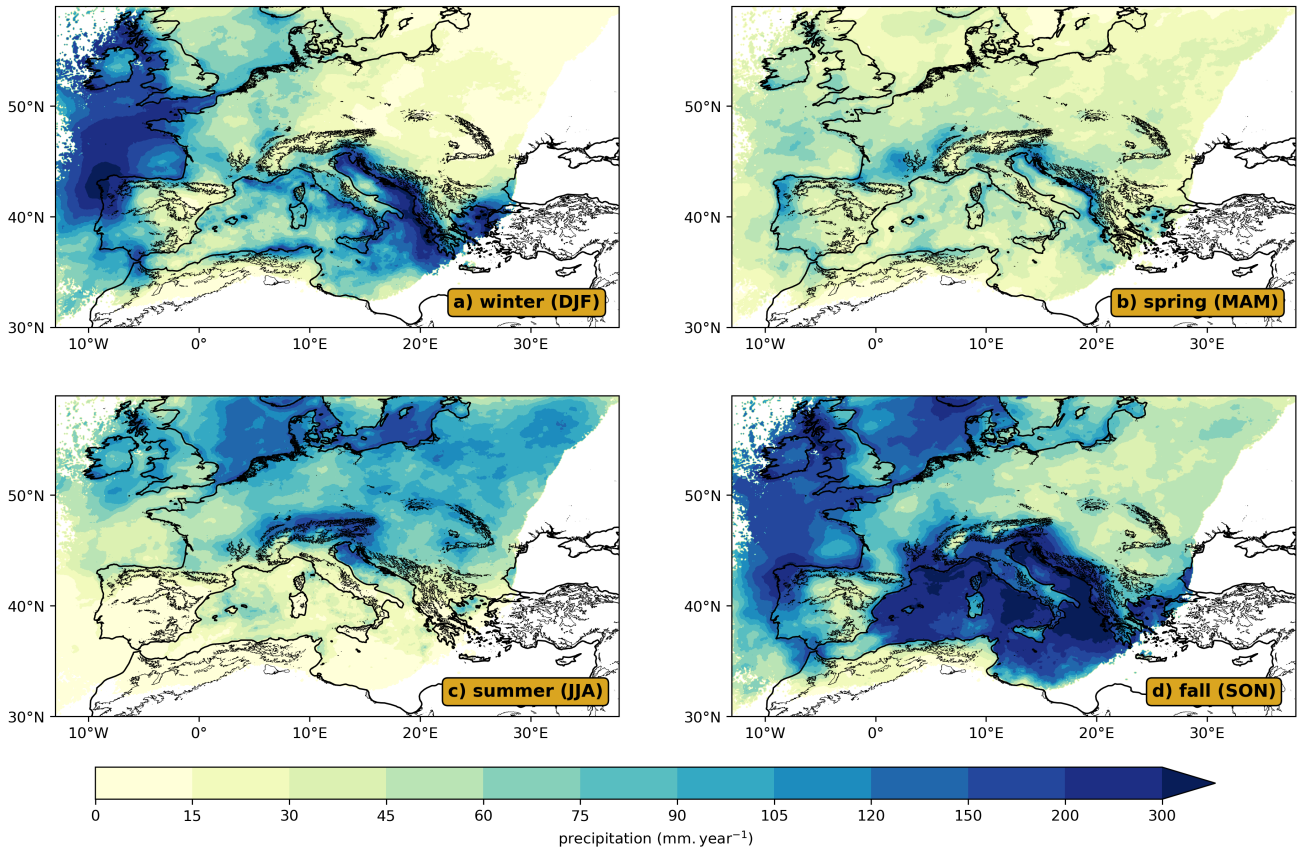
Figure S3.   Total precipitation per year from MCS identified based on the alternative CAPE method (text S1) over Europe in winter (DJF, a), spring (MAM, b), summer (JJA, c) and fall (SON, d).
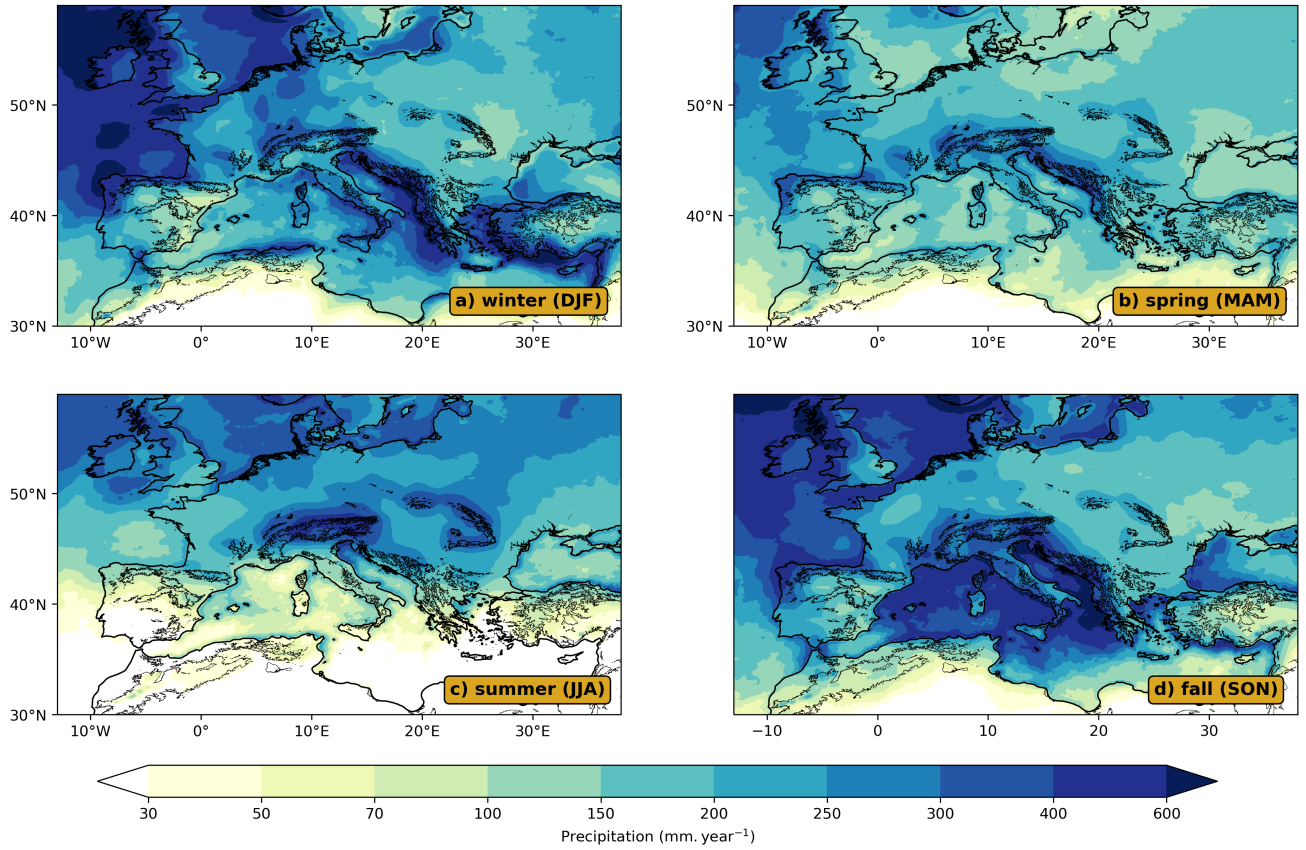
Figure S4. Total IMERG precipitation climatology (from 2001 to 2020; in mm.year^{-1}) over Europe in winter (DJF, a), spring (MAM, b), summer (JJA, c) and fall (SON, d).
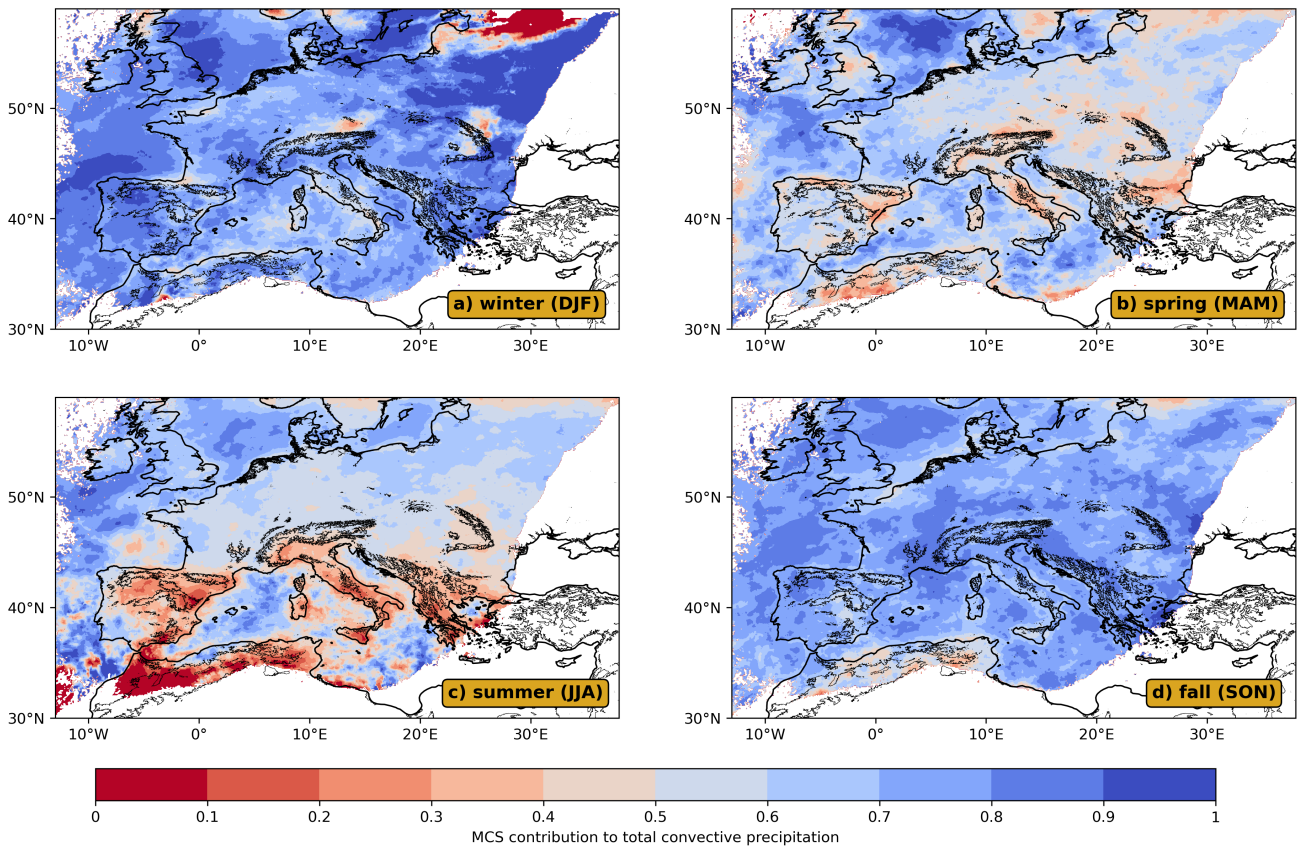
Figure S5. Contribution of MCS to convective precipitation over Europe in winter (DJF, a), spring (MAM, b), summer (JJA, c) and fall (SON, d).
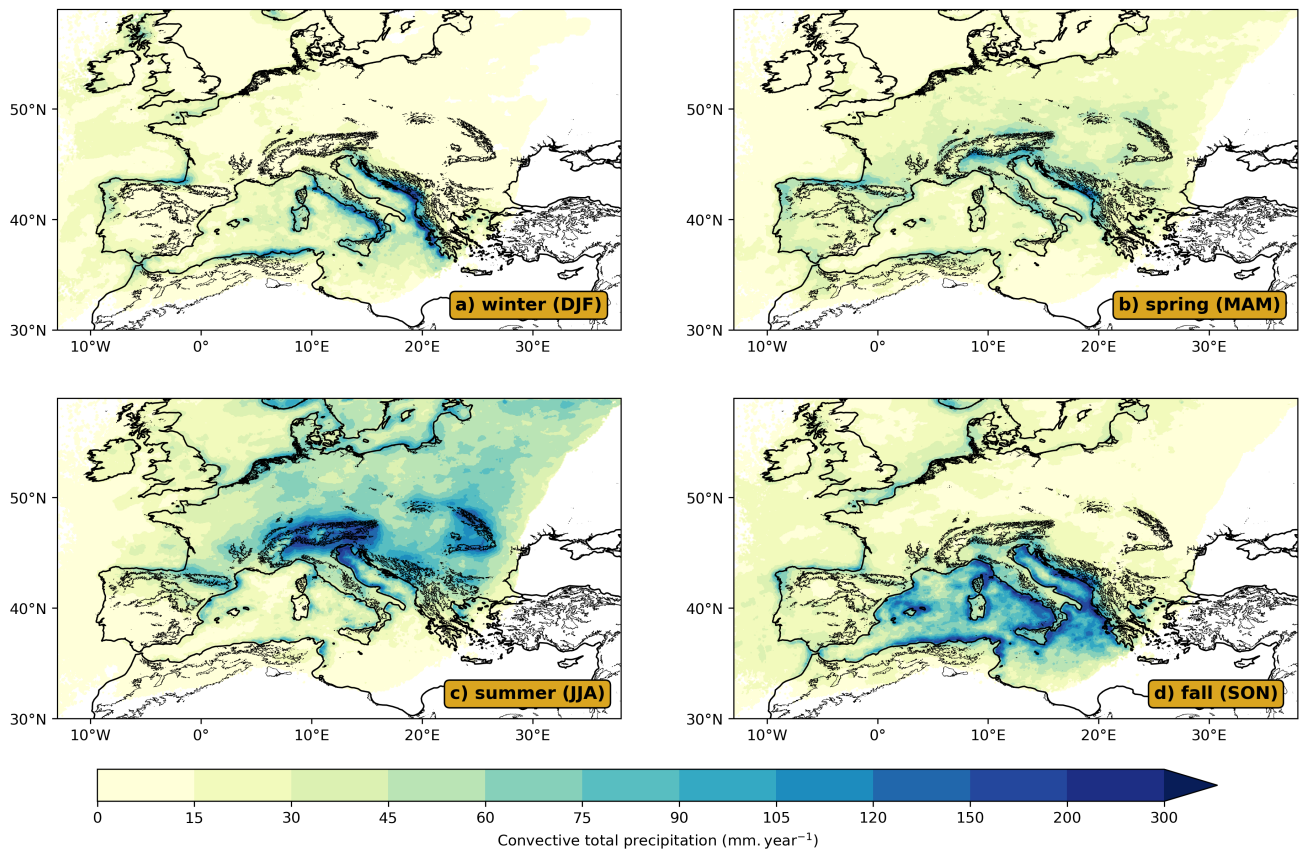
Figure S6. Total precipitation per year (in mm.year^{-1}) from isolated convective PFs over Europe in winter (DJF, a), spring (MAM, b), summer (JJA, c) and fall (SON, d).

April 10, 2023, 12:09pm

:
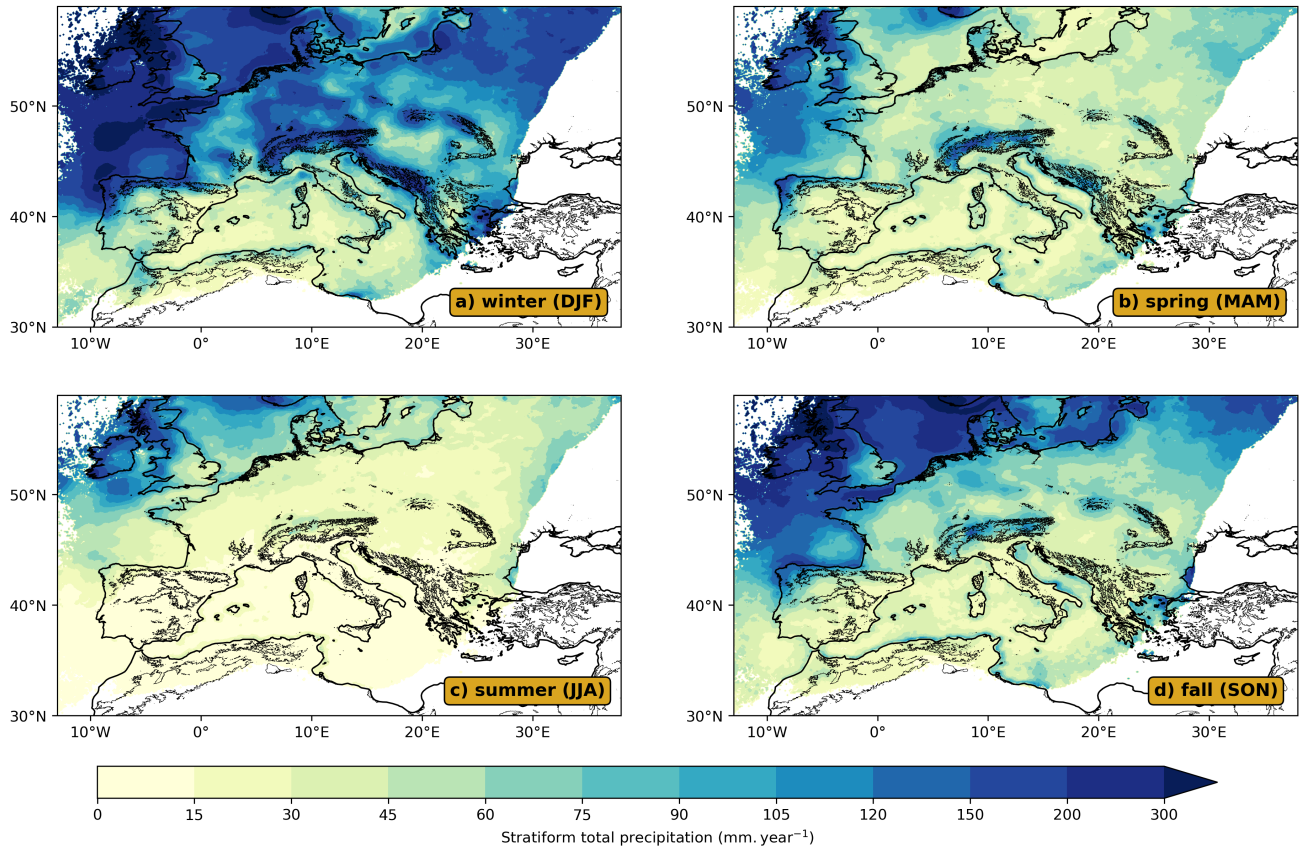
Figure S7.   Total precipitation per year (in mm.year^{-1}) from stratiform PFs over Europe in winter (DJF, a), spring (MAM, b), summer (JJA, c) and fall (SON, d). White areas represent missing values, defined as points with means of less than one lightning strike per year.
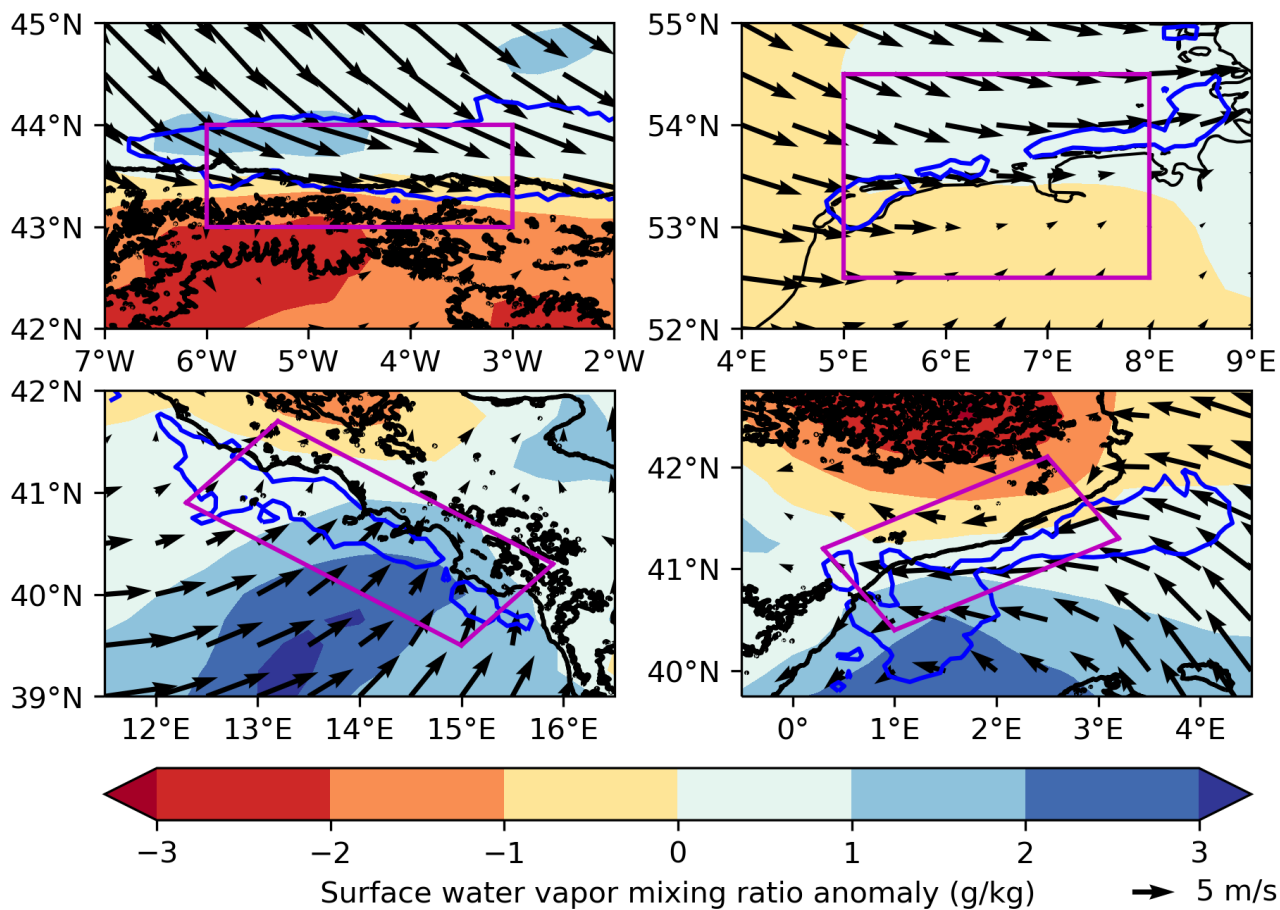
Figure S8. Surface water vapor mixing ratio (shadings) and wind (arrows) monthly anomalies for isolated convection coastal precipitation events (inside the magenta box) in December over the coasts of northern Spain (a), Netherlands and Germany (b), western Italy (c) and eastern Spain (d). Blue contours delimit areas where isolated convection mean precipitation is above 0.5 mm for these events.

April 10, 2023, 12:09pm

:
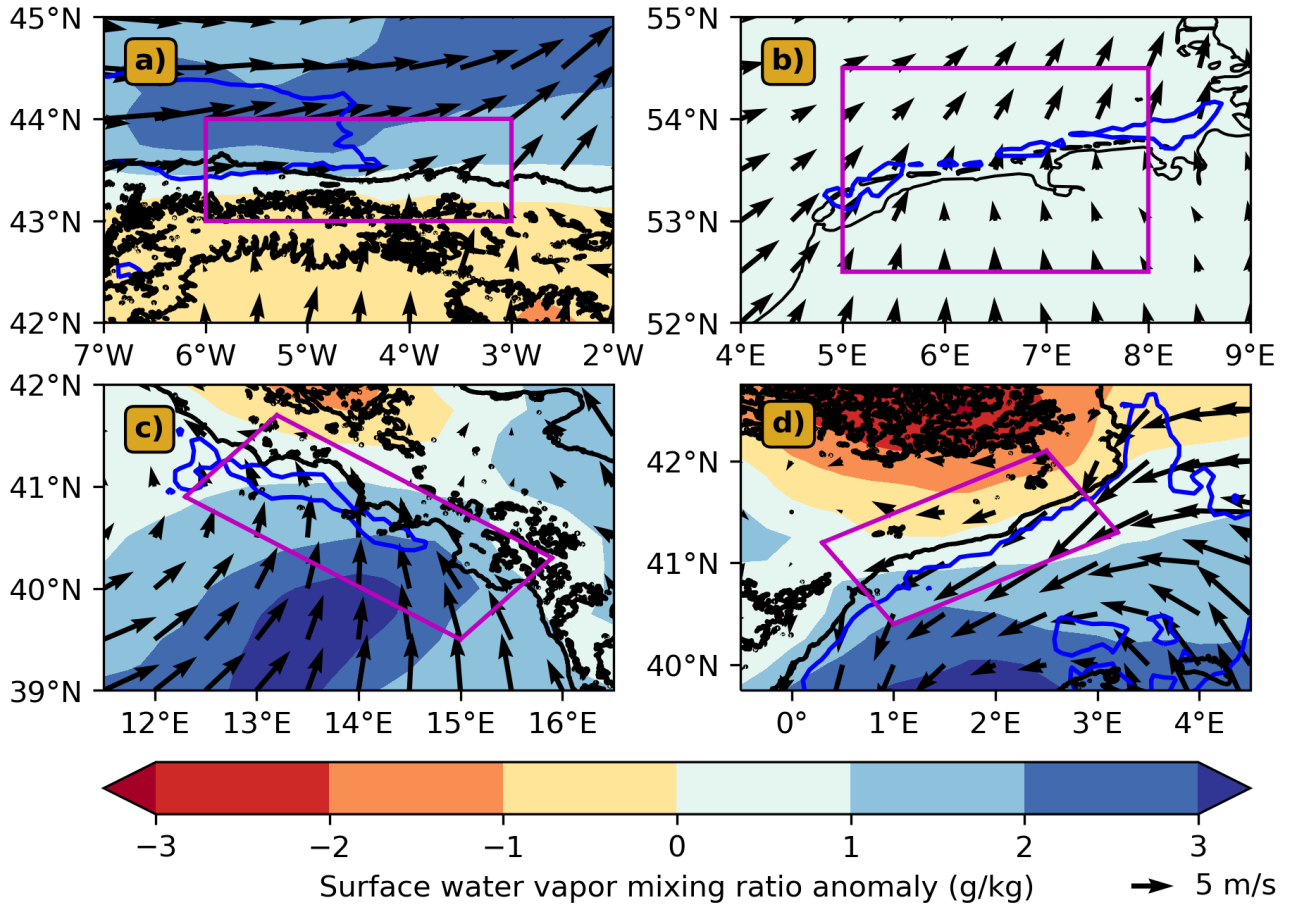
Figure S9. Surface water vapor mixing ratio (shadings) and wind (arrows) monthly anomalies for MCS coastal precipitation events (inside the magenta box) in December over the coasts of northern Spain (a), Netherlands and Germany (b), western Italy (c) and eastern Spain (d). Blue contours delimit areas where MCS mean precipitation is above 2 mm for these events.
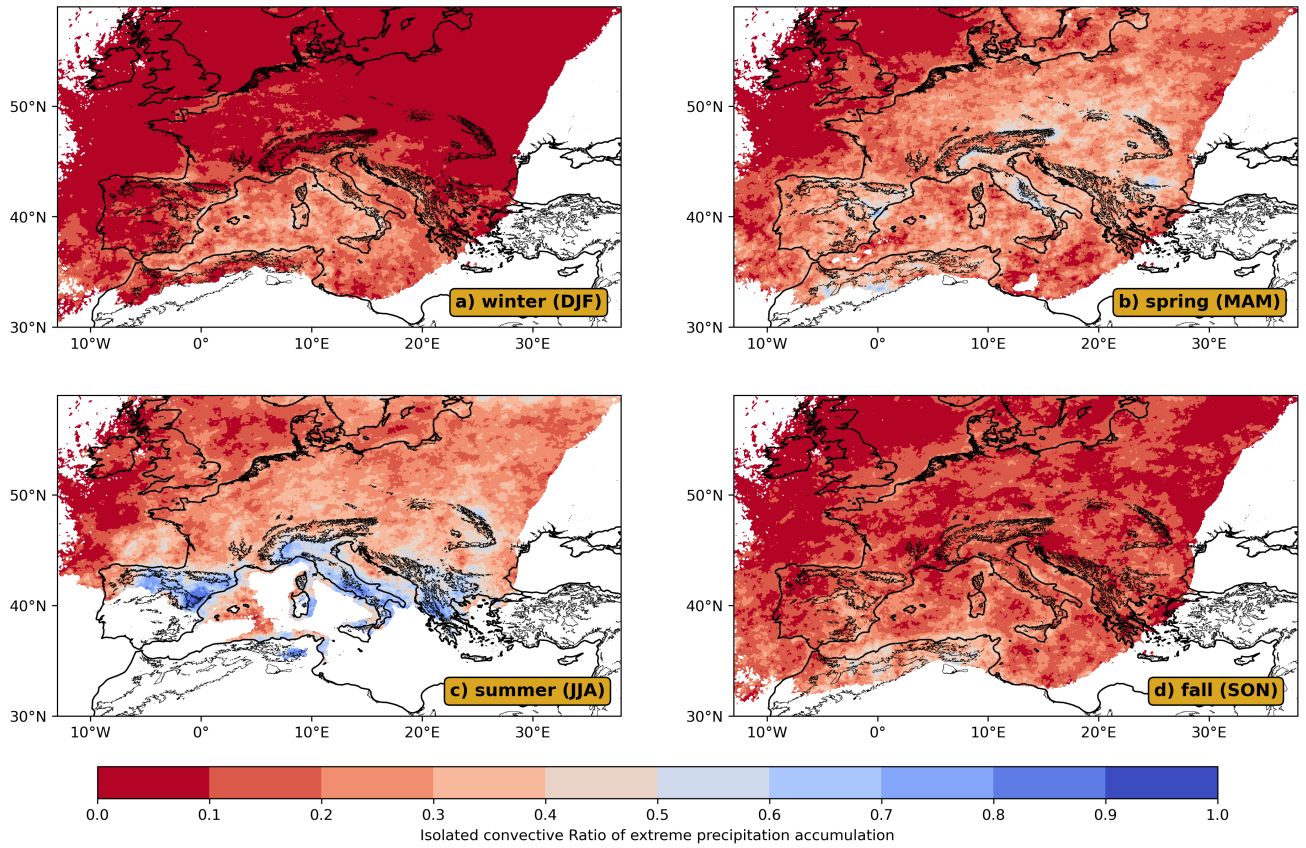
Figure S10. Contribution of isolated convection to the precipitation features producing the 10% most extreme precipitation accumulations (as defined in section 3.4) over Europe in winter (DJF, a), spring (MAM, b), summer (JJA, c) and fall (SON, d).

:
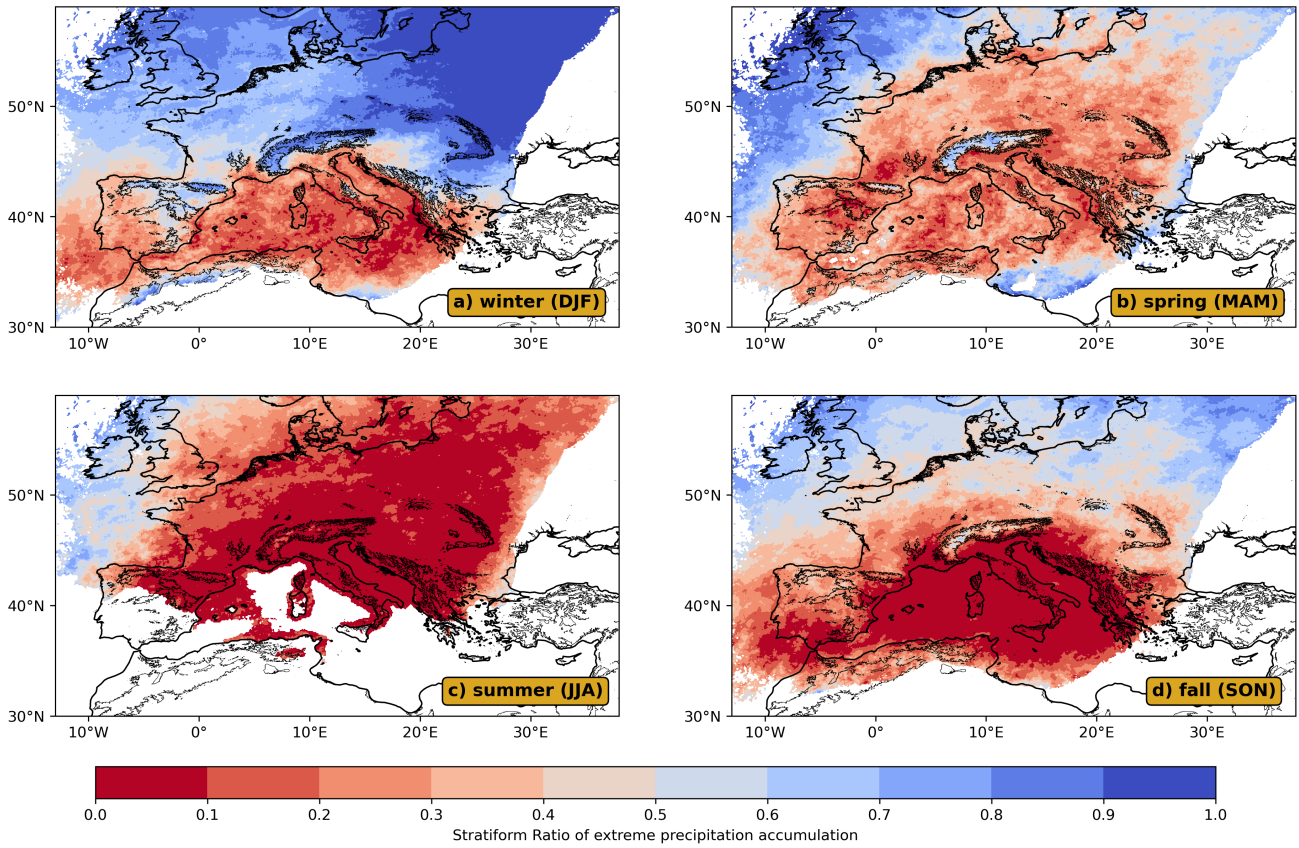
Figure S11. Contribution of stratiform events to the precipitation features producing the 10% most extreme precipitation accumulations (as defined in section 3.4) over Europe in winter (DJF, a), spring (MAM, b), summer (JJA, c) and fall (SON, d).
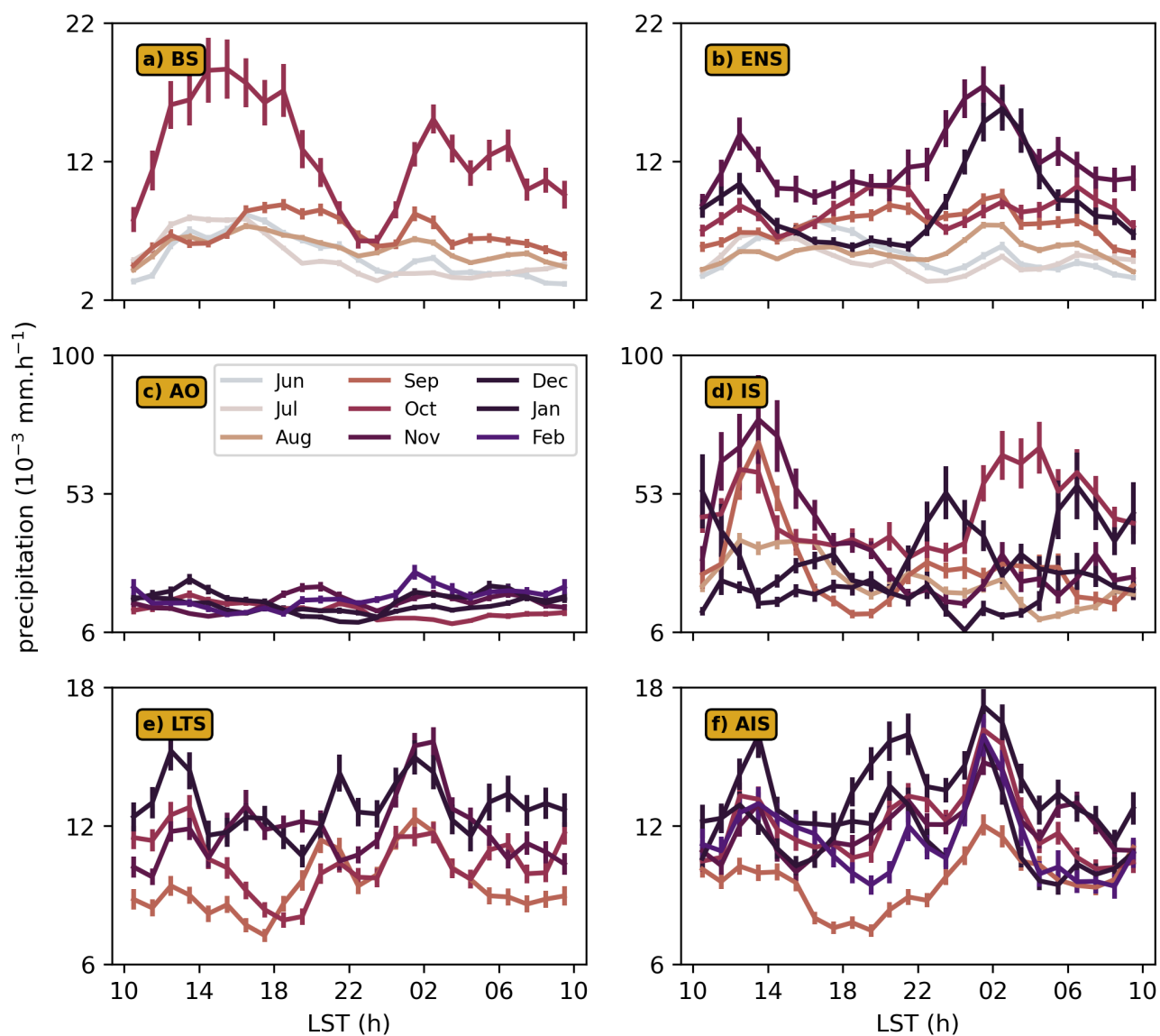
Figure S12. Monthly expected values of isolated convective precipitation (in mm.h^{-1}) conditioned on isolated convection occurrence within the coastal sub-regions as a function of LST: BS (a), ENS (b), AO (c), IS (d), LTS (e) and AIS (f) (see Fig. 3 of the main manuscript). Results are given for months with the main MCS activity according to Fig. 4 of the main manuscript. For each LST bin the standard error is calculated to estimate the uncertainty in the mean and represented by error bars.

April 10, 2023, 12:09pm
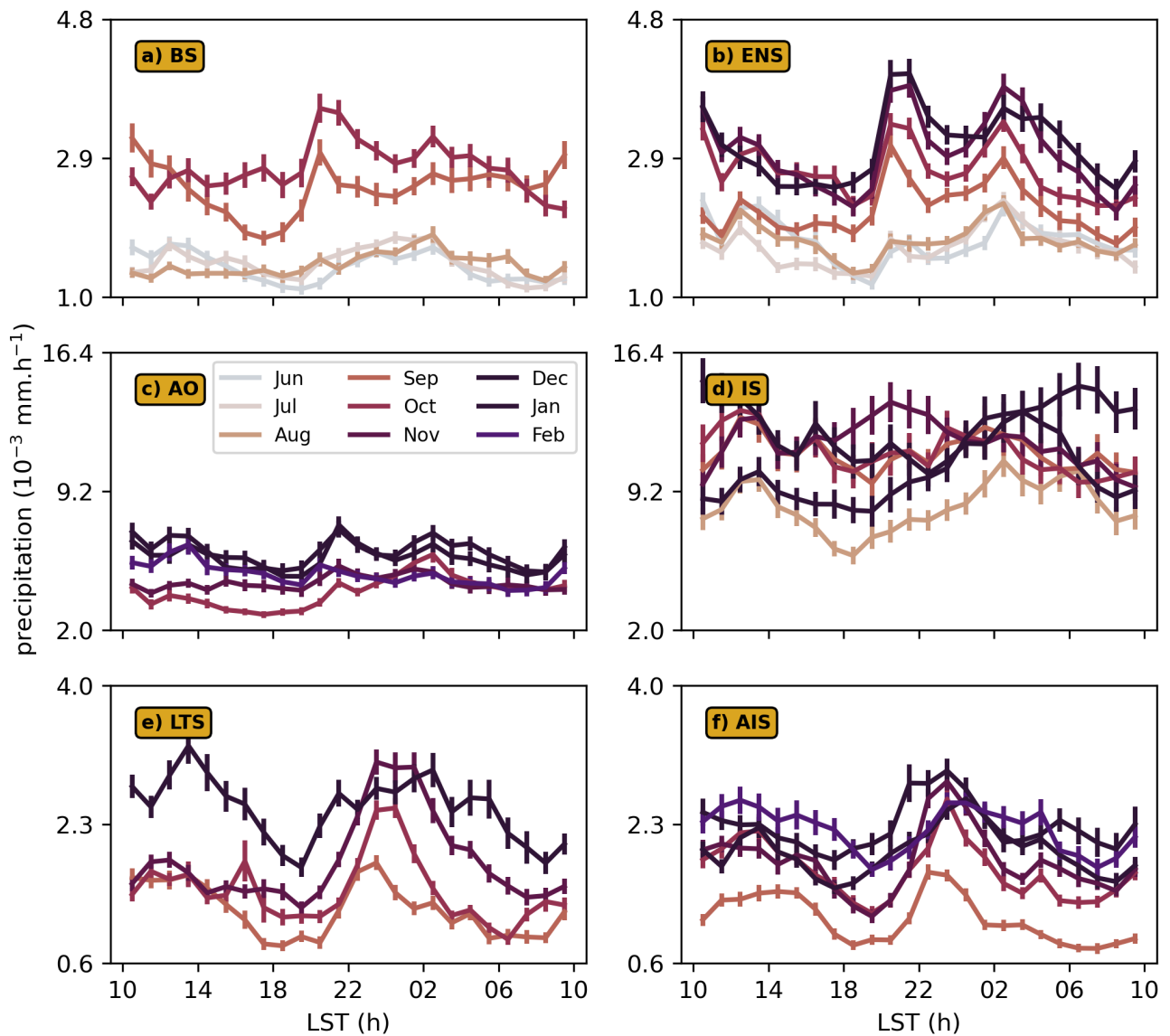
Figure S13. Monthly expected values of stratiform precipitation (in mm) conditioned on stratiform precipitation occurrence within the coastal sub-regions as a function of LST: BS (a), ENS (b), AO (c), IS (d), LTS (e) and AIS (f) (see Fig. 3 of the main manuscript). Results are given for months with the main MCS activity according to Fig. 4 of the main manuscript. For each LST bin the standard error is calculated to estimate the uncertainty in the mean and represented by error bars.
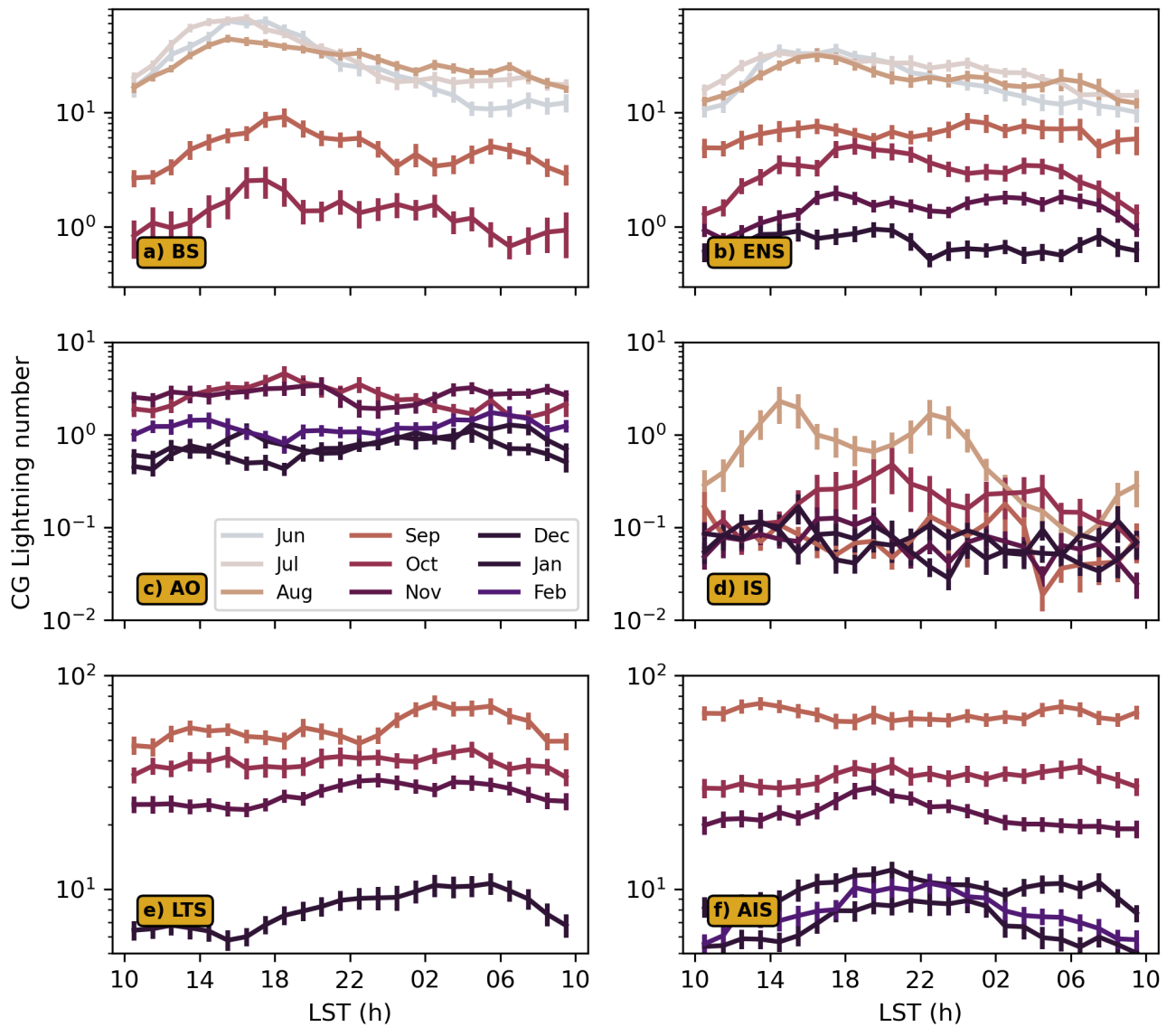
Figure S14. Monthly averaged diurnal cycle of EUCLID Cloud to Ground lightning strikes for the coastal sub-regions: BS (a), ENS (b), AO (c), IS (d), LTS (e) and AIS (f) (see Fig. 3 of the main manuscript).
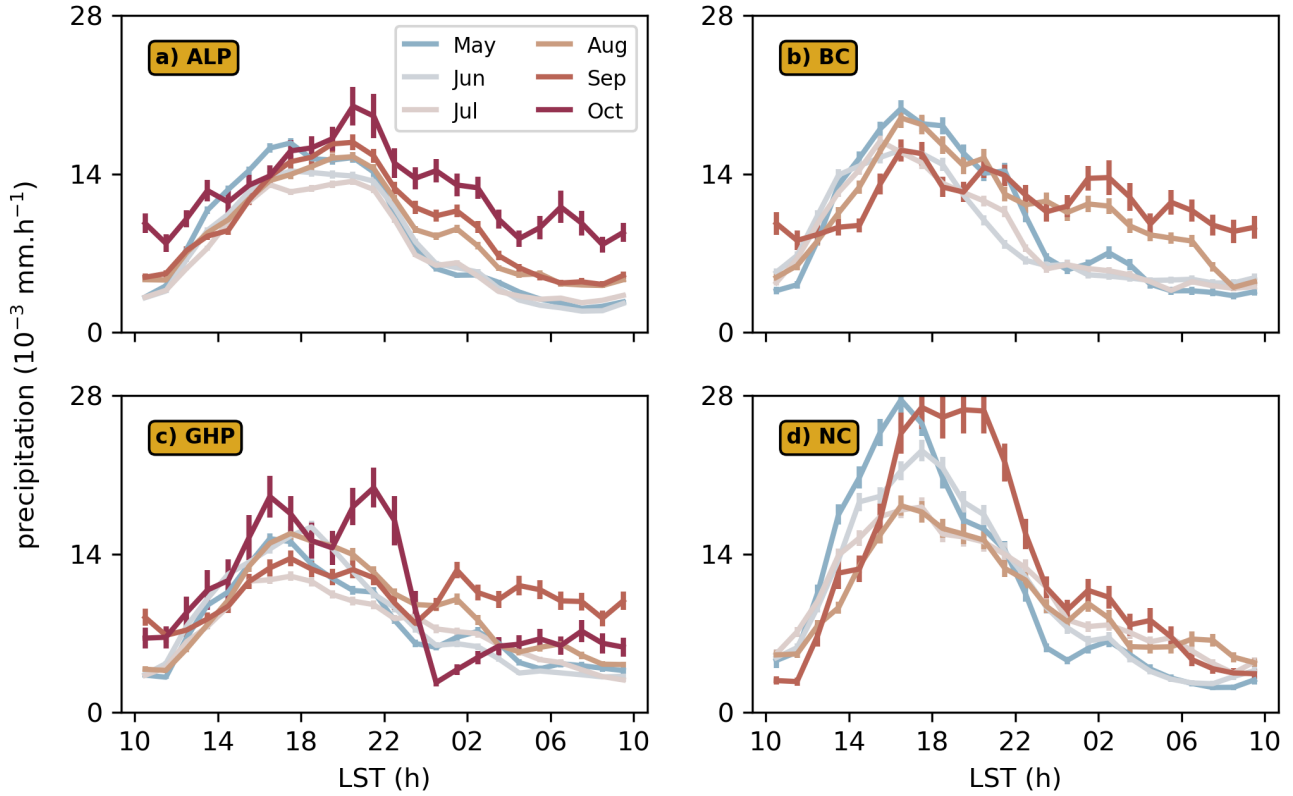
Figure S15. Monthly expected values of isolated convection precipitation (in mm.h^{-1}) conditioned on isolated convection occurrence within the continental sub-regions as a function of LST: ALP (a), BC (b), GHP (c) and NC (d) (see Fig. 3 of the main manuscript). Results are given for months with the main MCS activity according to Fig. 4 of the main manuscript. For each LST bin the standard error is calculated to estimate the uncertainty in the mean and represented by error bars.
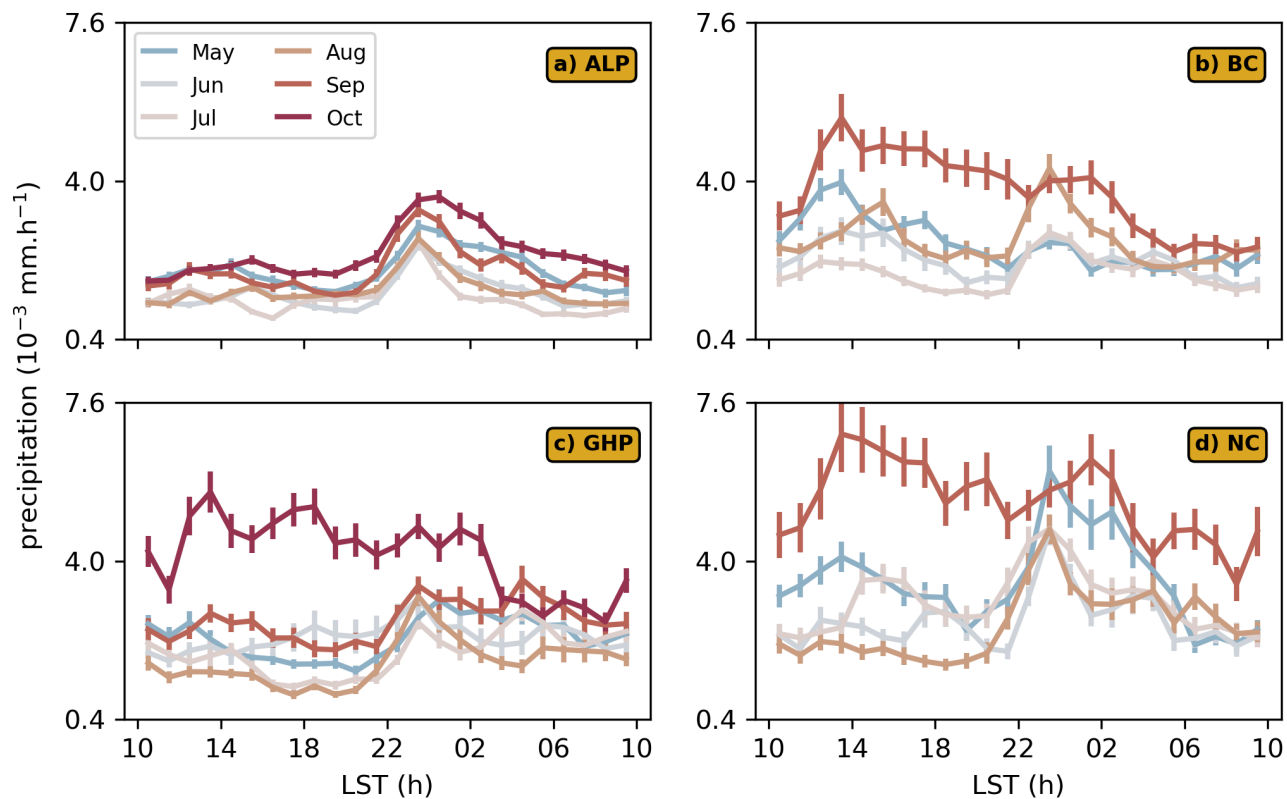
Figure S16. Monthly expected values of stratiform precipitation (in mm.h^{-1}) conditioned on stratiform precipitation occurrence within the continental sub-regions as a function of LST: ALP (a), BC (b), GHP (c) and NC (d) (see Fig. 3 of the main manuscript). Results are given for months with the main MCS activity according to Fig. 4 of the main manuscript. For each LST bin the standard error is calculated to estimate the uncertainty in the mean and represented by error bars.
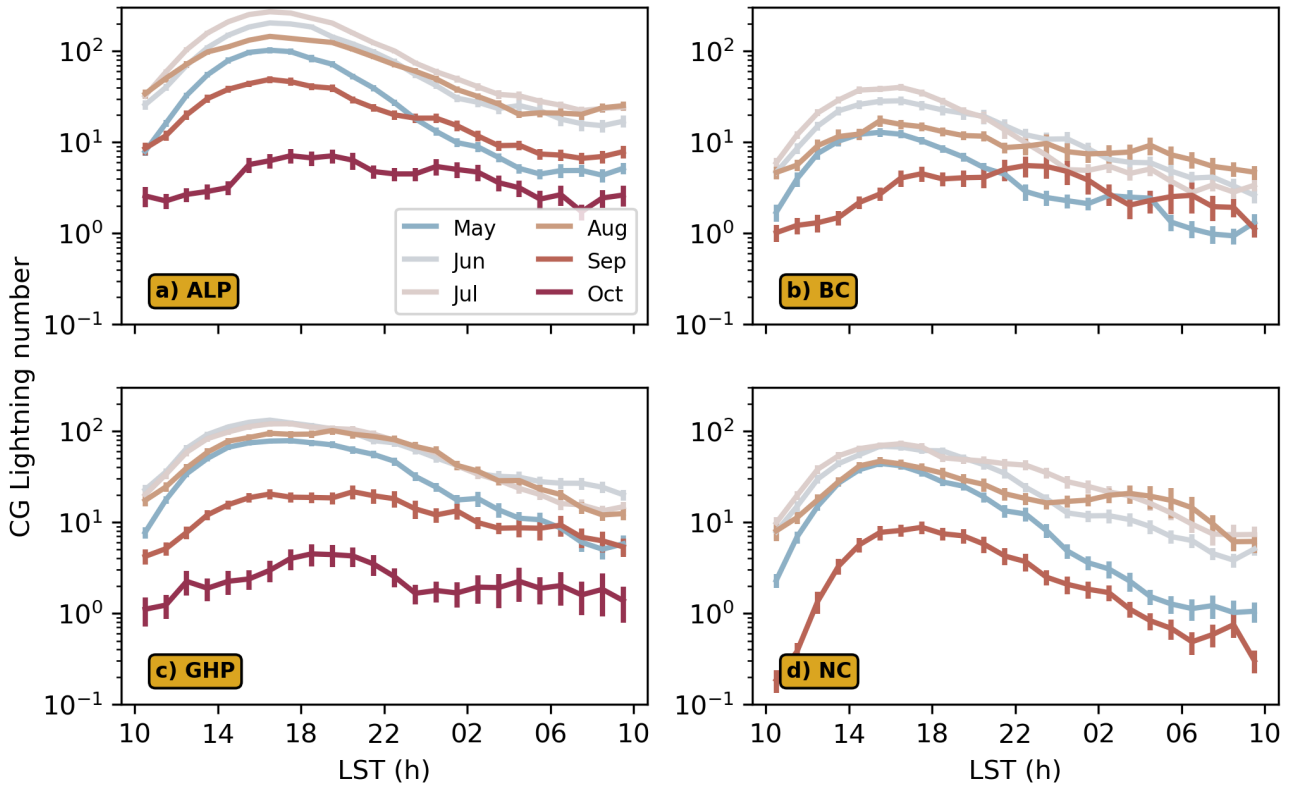
Figure S17.   Monthly averaged diurnal cycle of EUCLID Cloud to Ground lightning strikes for the continental sub-regions: ALP (a), BC (b), GHP (c) and NC (d) (see Fig. 3 of the main manuscript).
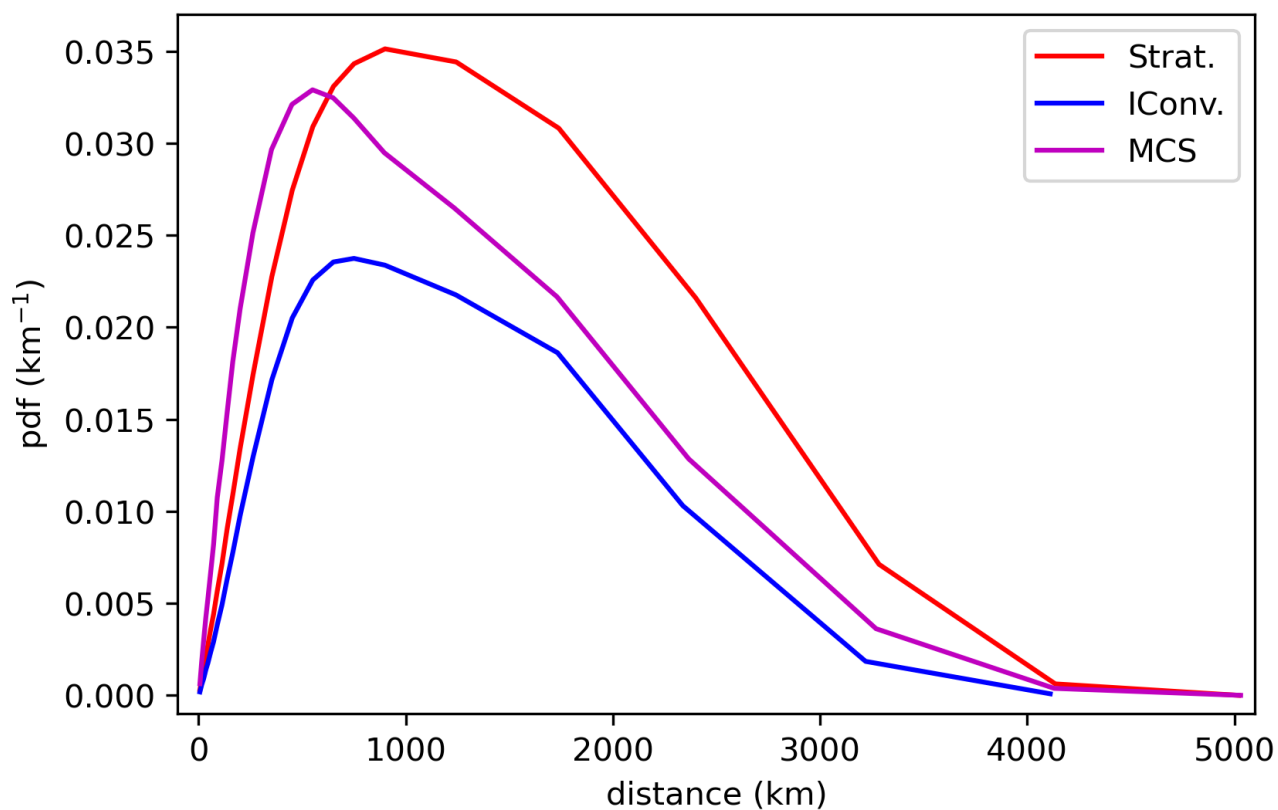
Figure S18. Unnormalized probability density functions (pdf) of frontal pixels as a function of distance from the center of every stratiform ("Strat.",red), isolated convective ("IConv", blue) and MCS (magenta) PFs at their maximum extent.